Sodium alginate assisted construction of $ZnSnO_3$ microspheres enhanced HCHO sensing performance under UV illumination at room temperature

Jie Chen, Zhihua Ying ✉, Peng Zheng, Rongfa Gao, Jinbang Mei

College of Electronics and Information, Hangzhou Dianzi University, Hangzhou 310018, People's Republic of China
✉ *E-mail: yingzh@hdu.edu.cn*

Published in Micro & Nano Letters; Received on 2nd April 2019; Revised on 13th July 2019; Accepted on 25th September 2019

The $ZnSnO_3$ microspheres were fabricated with water-soluble biopolymer sodium alginate (SA) as a crystal growth modifier under hydrothermal conditions. The gas-sensing properties of $ZnSnO_3$@SA were tested under the illumination of UV light at room temperature. The results showed that the $ZnSnO_3$@SA sensor exhibited better HCHO gas response than pristine $ZnSnO_3$ sensor, which was ascribed to the introduction of SA that changed the size distribution of the microspheres. Test results of HCHO gas with different concentrations indicated that the $ZnSnO_3$@SA sensor had a good linearity. This approach would provide a potential route for the HCHO sensor to work at room temperature. In addition, the sensing mechanism was also discussed.

1. Introduction: The metal oxide semiconductors are considered the most promising sensing materials, which plays a crucial role in monitoring harmful and toxic gases due to their simple fabrication, high gas-sensing properties and low cost [1–3]. $ZnSnO_3$, as a ternary metal oxide semiconductor, has attracted considerable attention to their application in gas sensors, moisture detectors and lithium-ion batteries [4–6]. Zeng *et al.* [4] successfully prepared hierarchical $ZnSnO_3$ nanocages using the simple surfactant-assisted hydrothermal processes and discussed improvement on the sensing of ethanol and HCHO; Fan *et al.* [7] obtained hollow $ZnSnO_3$ microspheres through cetyltrimethylammonium bromide assisted hydrothermal method, which showed good butane sensing performance. However, these sensors typically require high operating temperature above 200°C, which limits their application [4, 8]. Recently, UV irradiation has been used to reduce the operating temperature of metal oxide semiconductors sensors [9–11]. In addition, the gas sensing characteristics are greatly dependent on nanomaterials morphology and structures. Among the existing approaches for fabricating nanomaterials, hydrothermal synthesis is probably most attractive because of its low cost, facile procedure, mild reaction conditions and high yield for scale production. Many nanomaterials have been successfully fabricated in solution conditions via a simple hydrothermal process, such as hierarchically porous ZnO [12], SnO_2 nanorods [13] and $ZnSnO_3$ nanocages [4]. Sodium alginate (SA) is a naturally available carbohydrate polymer, and it is considered as a 'green' chemical agent because it is biodegradable and non-toxic, so it has been used as a structure-directing agent for the synthesis of metal oxide nanoparticles [14–16]. In this Letter, $ZnSnO_3$ microspheres with different SA concentration synthesised via hydrothermal method, and the properties of $ZnSnO_3$@SA film towards HCHO were observed under UV illumination at room temperature. It is worth mentioning that we used SA to change the size distribution of the $ZnSnO_3$ microspheres for the first time, and $ZnSnO_3$ can be used as a promising candidate in the room temperature gas sensor applications.

2. Experimental: The $ZnSnO_3$@SA microspheres were obtained by one-step hydrothermal method as follows: first, 0.01 mol sodium stannate was dissolved in 10 ml deionised water at the magnetic stirring condition, then 10 ml of SA aqueous solution was added; 0.01 mol zinc acetate was dissolved in 2 ml deionised water, to which 5 ml ammonia aqueous solution was added. Then, the above-mentioned two solutions were mixed under continuous stirring, put into a 50 ml Teflon-lined autoclave and heated to 160°C for 12 h. After being cooled down naturally, the precipitates were collected by centrifugation, washed with deionised water and ethanol in turn, and air-dried at room temperature. Finally, the as-obtained samples were heated at 500°C (heating rate of 4°C/min) for 3 h. The products with different concentration SA are denoted as $ZnSnO_3$, $ZnSnO_3$@2 g/l SA, $ZnSnO_3$@4 g/l SA, $ZnSnO_3$@6 g/l SA, respectively.

The above materials were dissolved in deionised water (20 mg/ml) and ultrasonicated for 30 min. The films were prepared using spray-deposited method on the interdigital electrodes as Fig. 1*a*, then they were heated at 400°C for 2 h. The test process of $ZnSnO_3$@SA sensors exposed to HCHO was illustrated in Fig. 1*b*. Mass flow controller (D08-2E, Sevenstar, Beijing) was used to dilute the HCHO (Wetry, Shanghai, 20 ppm in N_2) with clean air and deliver these gases to the sensor chamber, meanwhile the total gas flow rate was kept constant at 500 ml/min when the HCHO concentration was different from 1 to 20 ppm. The characteristics of the prepared devices were measured using Keithley 2010 Multimeter and recorded by a PC. Along with this, all the measurement results were illuminated by UV light (peak wavelength 365 nm) at room temperature in the dry air. It is worth mentioning that no response was observed for all these samples in presence of HCHO without UV illumination.

3. Results and discussion: The scanning electron microscope (SEM, JEOL, 6460) was used to observe the morphologies of samples, and X-ray diffraction (XRD, Ultima IV) was employed to characterise the crystalline phases of all synthesised samples.

As observed in Fig. 2, the $ZnSnO_3$@SA materials showed microspheres in different sizes. The sizes of $ZnSnO_3$ and $ZnSnO_3$@6 g/l SA microspheres have broad distributions, most varied from 0.2 to 2.2 μm, with average diameters of 1.16 and 1.32 μm, respectively. Meanwhile, for $ZnSnO_3$@2 g/l SA and $ZnSnO_3$@4 g/l SA microspheres, the size of most particles centralised distributed from 0.6 to 1 μm, and the average size of particles is a little smaller than that of $ZnSnO_3$ microspheres, 1.09 and 0.94 μm, respectively. From the above results, it is presumable that the presence of SA could alter the assembly pattern of $ZnSnO_3$ nanoparticle.

The XRD patterns of the $ZnSn(OH)_6$ precursors are depicted in Fig. 3. As shown, all the sharp diffraction peaks can be indexed to the standard diffraction pattern of $ZnSn(OH)_6$ (PDF#73-2384). No diffraction peaks from any other phases can be detected, which indicates that the obtained precursors are pure $ZnSn(OH)_6$.

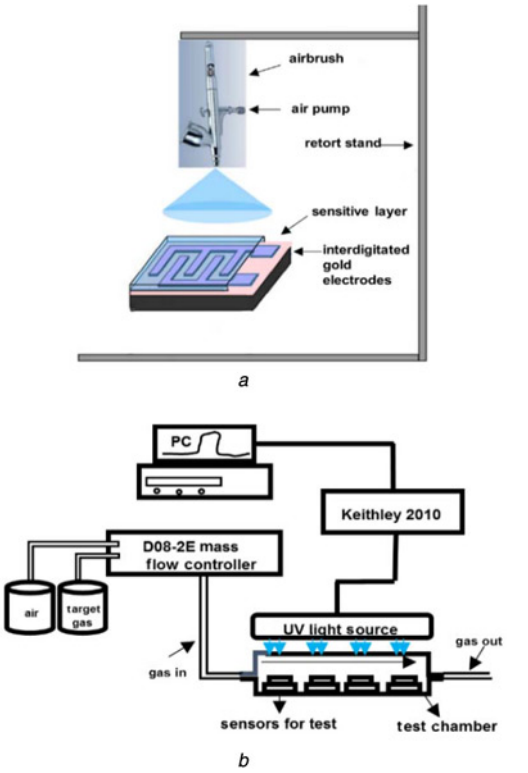

Fig. 1 *Schematic diagram of the device and test process*
a Device for deposited sensitive layer on the interdigitated gold electrodes
b Gas-sensing test system

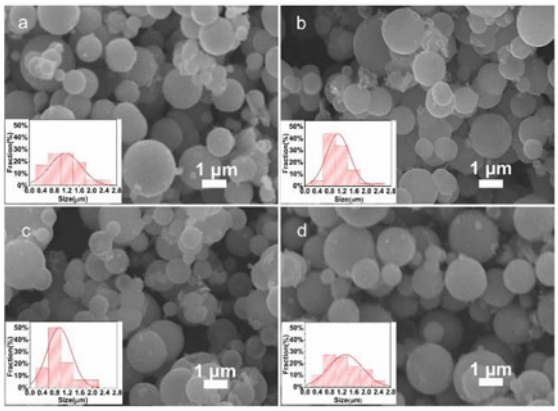

Fig. 2 *SEM images of the samples with the size distribution shown in the inset*
a $ZnSnO_3$
b $ZnSnO_3$@2 g/l SA
c $ZnSnO_3$@4 g/l SA
d $ZnSnO_3$@6 g/l SA

The dynamic response curves of the coated electrodes exposed to different concentrations of HCHO gas are shown in Fig. 4*a*. The response of the sensors is defined as the ratio of R_a/R_g, where R_a is the resistance of the gas sensor balanced in ambient air and R_g is the resistance in test gas (both with UV illumination). In the test cycle of each concentration, the HCHO response time is 150 s, then the dry air is introduced. With the SA amount being increased, the response increased correspondingly. It is obvious that all the $ZnSnO_3$@SA sensors exhibited higher sensitivity than $ZnSnO_3$ sensor, and among them the best one is $ZnSnO_3$@4 g/l SA sensor, which is nearly two-fold larger response obtained than the pristine one. Meanwhile, the curve of responses against

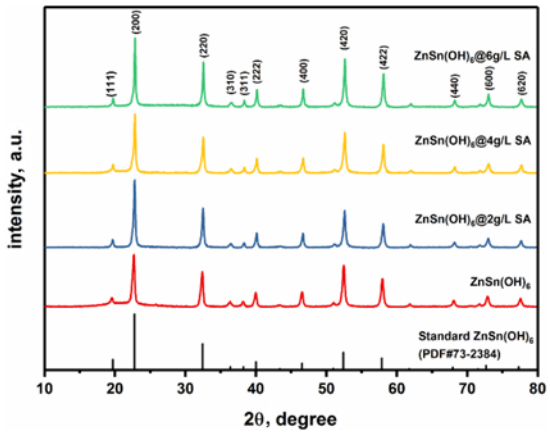

Fig. 3 *XRD patterns of $ZnSn(OH)_6$, $ZnSn(OH)_6$@2 g/l SA, $ZnSn(OH)_6$@4 g/l SA, $ZnSn(OH)_6$@6 g/l SA*

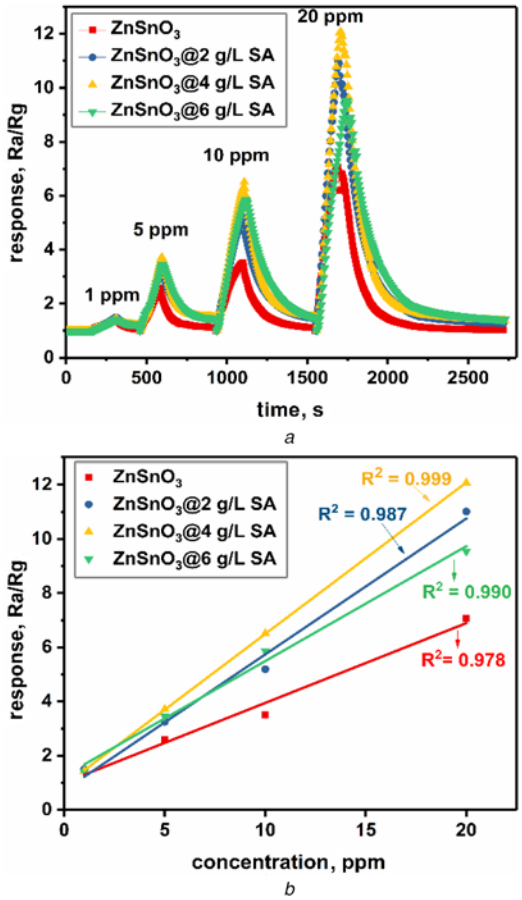

Fig. 4 *Test results with the $ZnSnO_3$@SA sensors*
a Real-time response to different concentrations HCHO under UV illumination at room temperature
b Response linear fittings

concentrations of HCHO gas was plotted in Fig. 4*b*. An excellent linearity of response to HCHO, which can be observed by the regression coefficient, shows all the sensors are >0.97. This is especially shown in the $ZnSnO_3$@4 g/l SA sensor at 0.99998, indicating that the ZnSnO3@SA sensor may be used as quantitative detection of HCHO vapour.

For comparison, some other works about $ZnSnO_3$-based HCHO gas detection in recent years are summarised in Table 1. The sample prepared in this study can detect HCHO sensing performance at

doi: 10.1049/mnl.2019.0207

Table 1 Summary of the HCHO sensors based on $ZnSnO_3$

Material	Morphology	Conc., ppm	Temp., °C	Response
$ZnSnO_3$	nanocages	50	260	17 [17]
$ZnSnO_3$	nanocages	50	350	57.6 [4]
$ZnSnO_3$	multishelled cubes	100	220	37.2 [18]
$ZnSnO_3$/rGO	microspheres	10	110	12 [19]
SnO_2@SA	microspheres	200	170	15 [14]
$ZnSnO_3$@SA	microspheres	20	room temperature	12.5 (this work)

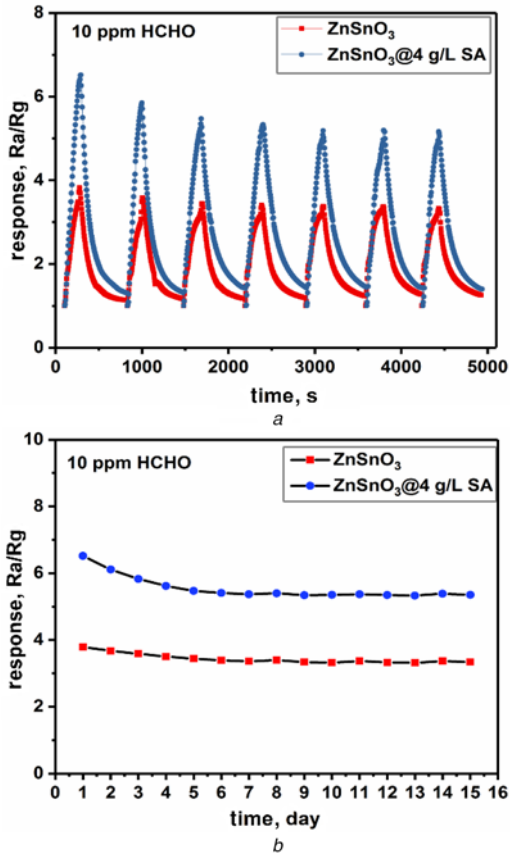

Fig. 5 *Sensors based on $ZnSnO_3$ and $ZnSnO_3$@4 g/l SA towards 10 ppm HCHO at room temperature*
a Seven repetitions of response curve
b Sensing stability of the samples for 15 days

room temperature, such a low operating temperature has not been reported so far for $ZnSnO_3$-based sensors. Moreover, compared with those HCHO sensors of pristine $ZnSnO_3$ under high operating temperatures, our prepared sensor exhibits approximative sensing performances with UV illumination even at the room temperature.

In addition, the cyclic response curve of the sensor based on $ZnSnO_3$@4 g/l SA exposed to 10 ppm HCHO for seven times is displayed in Fig. 5*a*. It can be found that the response has declined for the first few cycles, but then it gradually kept constant, which remains nearly 80% of its maximum sensitivity, where we can make a conscious effort to improve in the future. Not only the repeatability is very essential to a gas sensor, but also the stability is an important indicator in practice. The long-time stability of the gas sensor was measured every day at room temperature as shown in Fig. 5*b*. After 15 days measurement, despite of the first 5 days slightly decrease, the response of sensor based on $ZnSnO_3$@4 g/l SA still maintained at a stable value, which was always higher than the pristine $ZnSnO_3$. These indicated the sensor has a relatively stable character and might be a good candidate for the practical detection.

The sensing mechanism of the semiconductor gas sensor that is widely accepted is the change of the depletion layer taken place in the surface of the materials, which depends on the absorption and desorption of gas molecules [1, 2, 8]. When the sensors based on $ZnSnO_3$ were in the air, oxygen molecules were absorbed on the surface of materials that would trap electrons and translate into reactive oxygen ions (O^-, O_2^-), which formed a depletion layer in the surface region of the $ZnSnO_3$ and thus increased the resistance. Upon exposure to UV light, electron–hole pairs will be generated in $ZnSnO_3$, meanwhile some photo-generated electrons and holes may be recombined.

On the one hand, the remaining holes can reach the surface of $ZnSnO_3$ which will react with oxygen ions, leading to the width of the surface depletion layer being reduced and this causes the resistance to be decreased. On the other hand, the remaining photo-generated electrons can react with ambient oxygen molecules, leading to photo-induced oxygen ions [20]. When the sensors are exposed to HCHO gas, the chemical reactions between the photo-induced oxygen ions and formaldehyde molecules may happen, making the width of the surface depletion layer further reduced with electrons released according to the following equation:

$$\mathrm{HCHO(gas)} + \mathrm{O^-(ads)} \rightarrow \mathrm{H_2O(gas)} + \mathrm{CO_2(gas)} + e^- \quad (1)$$

Also, the properties of metal semiconductor oxide gas sensor are influenced by several factors, such as microstructure, porosity and impurities [10, 14]. The response of the sensor can be increased significantly by changing the microstructure like particle size. As the particles size decreases, a higher specific surface area is obtained, resulting in a large number of active sites, which facilitates gas adsorption and consequently for a higher sensitivity [21]. It has good consistency with our results shown in SEM. By introducing the SA of 4 g/l, the size of most $ZnSnO_3$ microspheres decreased obviously and concentrated from 0.8 to 1 μm, so the $ZnSnO_3$@4 g/l SA sample expressed a superior response to HCHO. Although the smaller grain size is better for the sensitivity of gas sensors, excessive reduction in grain size reduces structural stability [22], which resulting in the stability of this HCHO sensor needs to be improved in the future.

4. Conclusion: In summary, we reported a HCHO sensor based on biopolymer-assisted synthesised $ZnSnO_3$ microspheres, which were prepared by a simple hydrothermal route. UV illumination made this HCHO sensor response at room temperature into realisation. The sensors coated with $ZnSnO_3$@SA films towards 20 ppm HCHO presented nearly more than twice of the sensors based on $ZnSnO_3$ films, which may be ascribed to the introduction of SA changed the size distribution of the materials. In addition, the $ZnSnO_3$@SA sensor exhibited a good linearity despite of its unsatisfactory repeatability, and a relative stability also can be observed in 15 days. We believe this research will promote the development of HCHO gas sensors under room temperature with further work.

5. Acknowledgment: This work was supported by the Natural Science Foundations of Zhejiang Province (grant no. LY17F010021) and Key Research and Development Program of Zhejiang Province (grant no. 2019C04003). Authors are thankful to Sam Jones for the kind help in proofreading this paper.

6 References

[1] Hu J., Wang T., Wang Y.J., *ET AL.*: 'Enhanced formaldehyde detection based on Ni doping of SnO_2 nanoparticles by one-step synthesis', *Sens. Actuators B.*, 2018, **263**, pp. 120–128

[2] Pan F.J., Lin H., Zhai H.Z., *ET AL.*: 'Pd-doped TiO_2 film sensors prepared by premixed stagnation flames for CO and NH_3 gas sensing', *Sens. Actuators B.*, 2018, **261**, pp. 451–459

[3] Shen J.Y., Zhang L., Ren J., *ET AL.*: 'Highly enhanced acetone sensing performance of porous C-doped WO_3 hollow spheres by carbon spheres as templates', *Sens. Actuators B.*, 2017, **239**, pp. 597–607

[4] Zeng Y., Zhang T., Fan H.T., *ET AL.*: 'Synthesis and gas-sensing properties of $ZnSnO_3$ cubic nanocages and nanoskeletons', *Sens. Actuators B.*, 2009, **143**, pp. 449–453

[5] Wang Y., Gao P., Bao D., *ET AL.*: 'One pot, two phases: individual orthorhombic and face-centered cubic $ZnSnO_3$ obtained synchronously in one solution', *Inorg. Chem.*, 2014, **53**, pp. 12289–12296

[6] Xie Q.S., Ma Y.T., Zhang X.Q., *ET AL.*: 'Synthesis of amorphous $ZnSnO_3$-C hollow microcubes as advanced anode materials for lithium ion batteries', *Electrochim. Acta*, 2014, **141**, pp. 374–383

[7] Fan H.T., Zeng Y., Xu X.J., *ET AL.*: 'Hydrothermal synthesis of hollow $ZnSnO_3$ microspheres and sensing properties toward butane', *Sens. Actuators B.*, 2011, **153**, pp. 170–175

[8] Bing Y.F., Zeng Y., Liu C., *ET AL.*: 'Assembly of hierarchical $ZnSnO_3$ hollow microspheres from ultra-thin nanorods and the enhanced ethanol-sensing performances', *Sens. Actuators B.*, 2014, **190**, pp. 370–377

[9] Meng L.X., Xu Q., Sun Z., *ET AL.*: 'Enhancing the performance of room temperature ZnO microwire gas sensor through a combined technology of surface etching and UV illumination', *Mater. Lett.*, 2018, **212**, pp. 296–298

[10] Gao R.F., Ying Z.H., Sheng W.Q., *ET AL.*: 'Gas sensors based on ZnO/silk fibroin film for nitrogen dioxide detection under UV light at room temperature', *Mater. Lett.*, 2018, **229**, pp. 210–212

[11] Da Silva L.F., M'Peko J.C., Catto A.C., *ET AL.*: 'UV-enhanced ozone gas sensing response of ZnO-SnO_2 heterojunctions at room temperature', *Sens. Actuators B.*, 2017, **240**, pp. 573–579

[12] Liu X.H., Zhang J., Wang L.W., *ET AL.*: '3D hierarchically porous ZnO structures and their functionalization by Au nanoparticles for gas sensors', *J. Mater. Chem.*, 2011, **21**, pp. 349–356

[13] Wang S.R., Yang J.D., Zhang H.X., *ET AL.*: 'One-pot synthesis of 3D hierarchical SnO_2 nanostructures and their application for gas sensor', *Sens. Actuators B.*, 2015, **207**, pp. 83–89

[14] Jin P.P., Zou X.X., Zhou L.J., *ET AL.*: 'Biopolymer-assisted construction of porous SnO_2 microspheres with enhanced sensing properties', *Sens. Actuators B*, 2014, **204**, pp. 142–148

[15] Liu R.M., Jiang Y.W., Gao F., *ET AL.*: 'Biopolymer-assisted construction and gas-sensing study of uniform solid and hollow $ZnSn(OH)_6$ spheres', *Sens. Actuators B.*, 2013, **178**, pp. 119–124

[16] Chen Q., Ma S.Y., Jiao H.Y., *ET AL.*: 'Sodium alginate assisted hydrothermal method to prepare praseodymium and cerium co-doped $ZnSn(OH)_6$ hollow microspheres and synergistically enhanced ethanol sensing performance', *Sens. Actuators B.*, 2017, **252**, pp. 295–305

[17] Jia X., Tian M., Zhang Z., *ET AL.*: 'Highly sensitive formaldehyde chemical sensor based on in situ precipitation synthesis of ZnSnO3 microspheres', *J. Mater. Sci. Mater. Electron.*, 2015, **26**, pp. 6224–6231

[18] Zhou T. T., Zhang T., Zhang R., *ET AL.*: 'Hollow $ZnSnO_3$ cubes with controllable shells enabling highly efficient chemical sensing detection of formaldehyde vapors', *ACS Appl. Mater. Interfaces*, 2017, **9**, pp. 14525–14533

[19] Sun J., Bai S., Tian Y., *ET AL.*: 'Hybridization of $ZnSnO_3$ and rGO for improvement of formaldehyde sensing properties', *Sens. Actuators B.*, 2018, **257**, pp. 29–36

[20] Wang X.Y., Ding B.N., Liu Y.P., *ET AL.*: 'Synthesis of 3D flower-like $znSnO_3$ and improvement of ethanol-sensing properties at room temperature based on nano-TiO_2 decoration and UV radiation', *Sens. Actuators B.*, 2018, **264**, pp. 119–127

[21] Mirzaei A., Leonardi S.G., Neri G.: 'Detection of hazardous volatile organic compounds (VOCs) by metal oxide nanostructures-based gas sensors: A review', *Ceram. Int.*, 2016, **42**, pp. 15119–15141

[22] Dey A.: 'Semiconductor metal oxide gas sensors: a review', *Mater. Sci. Eng. B.*, 2018, **229**, pp. 206–217

doi: 10.1049/mnl.2019.0207